12

Quantifying Water Flow and Retention in an Unsaturated Fracture-Facial Domain

John R. Nimmo[1] and Siamak Malek-Mohammadi[2]

ABSTRACT

Hydrologically significant flow and storage of water occur in macropores and fractures that are only partially filled. To accommodate such processes in flow models, we propose a three-domain framework. Two of the domains correspond to water flow and water storage in a fracture-facial region, in addition to the third domain of matrix water. The fracture-facial region, typically within a fraction of a millimeter of the fracture wall, includes a flowing phase whose fullness is determined by the availability and flux of preferentially flowing water, and a static storage portion whose fullness is determined by the local matric potential. The flow domain can be modeled with the source-responsive preferential flow model, and the roughness-storage domain can be modeled with capillary relations applied on the fracture-facial area. The matrix domain is treated using traditional unsaturated flow theory. We tested the model with application to the hydrology of the Chalk formation in southern England, coherently linking hydrologic information including recharge estimates, streamflow, water table fluctuation, imaging by electron microscopy, and surface roughness. The quantitative consistency of the three-domain matrix-microcavity-film model with this body of diverse data supports the hypothesized distinctions and active mechanisms of the three domains and establishes the usefulness of this framework.

12.1. INTRODUCTION

There is much experimental evidence, for example, from *Tokunaga and Wan* [1997], *Su et al.* [1999], and *Dragila and Weisbrod* [2003] that partially filled pores contribute substantially to preferential as well as diffuse flow. Preferential flow is known to be critically important to contaminant-transport and water-resource issues, and its occurrence in unsaturated media is widespread [*Nimmo*, 2012]. An important feature is that because of reduced viscous friction from there being less solid surface in contact with the flowing liquid, flow in partially filled conduits can be faster than in totally filled conduits, as commonly noted in textbooks on fluid dynamics. Various researchers [e.g. *Tokunaga et al.*, 2000; *Tuller and Or*, 2001; *Hincapié and Germann*, 2009; *Nimmo*, 2010] have developed models based on partially filled pores.

[1] U.S. Geological Survey, Menlo Park, California, USA
[2] Bradley University, Peoria, Illinois, USA

Complications arise from the dominance of different physical processes affecting flow in the matrix and the fractures, given that observed hydrologic behavior results from their combination and the interaction between them. This poses a serious challenge to traditional unsaturated-zone flow theory, which emphasizes a binary filled/unfilled state of pores that either are or are not conducting flow. The unsaturated flow properties of a macroscopic medium are traditionally construed to result from the collective effect of those pores that are completely filled with water. *Celia et al.* [1995], *Or and Tuller* [1999], and others have noted that this construct, which neglects the hydraulic effect of partially filled pores, is overused in unsaturated zone hydrology.

In this chapter we discuss and quantify the dynamics of flow, replenishment, storage, and drainage of an unsaturated zone fracture-facial domain. Spatially, it comprises that portion of a fracture's internal volume typically within a fraction of a millimeter of the fracture's internal face, within which water flow and storage occur

Dynamics of Fluids and Transport in Complex Fractured-Porous Systems, Geophysical Monograph 210, First Edition.
Edited by Boris Faybishenko, Sally M. Benson, and John E. Gale.

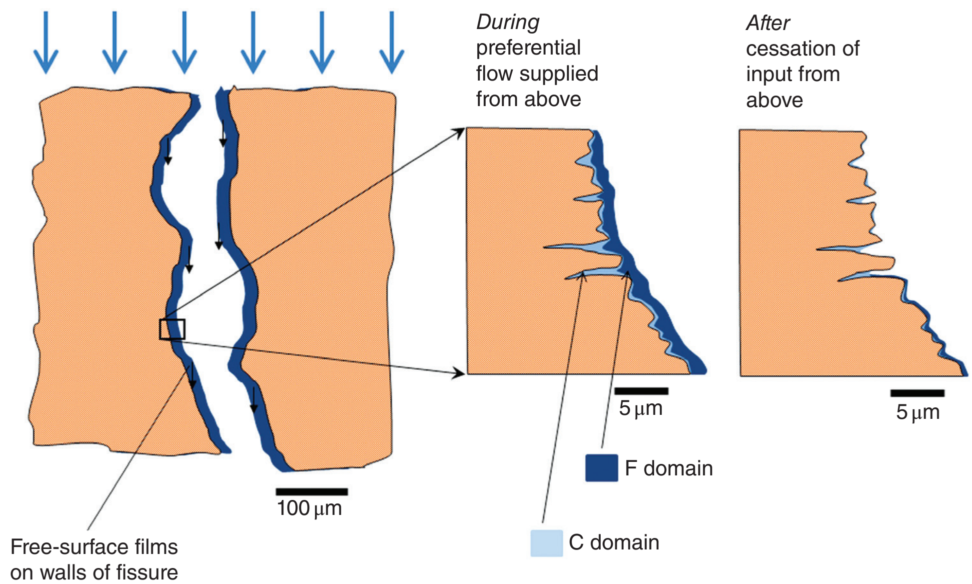

Figure 12.1 Diagram showing the C and F domains within a fissure. The two alternative inset drawings illustrate the configuration of C- and F-domain water during and after a major episode of preferential flow supplied from above.

while the fracture is not completely water filled. The overriding practical question is how can matric potentials, saturation state, and flowing water associated with matrix and fracture domains be reconciled with each other and with observed behavior at timescales of storms, seasons, and unsaturated-zone residence. Although some terminology here pertains primarily to fractured rock, the content may also relate to the analogous case of macroporous soil and other media with the possibility of unsaturated preferential flow. In this chapter we use the term *fracture* to refer to any possible nonmatrix flow conduit, regardless of shape or developmental process.

Objectives of this chapter center on development of a model based on films and microcavities that quantitatively accounts for both water flow and storage in the fracture-facial region. This model must relate to pores in matrix material that may or may not participate in water transport and with which it is not necessarily in equilibrium. We have tested this model with available data from lab experiments and field observations to evaluate whether it can provide a coherent, self-consistent quantification of hydrologically important phenomena associated with unsaturated-zone preferential flow.

12.2. HYDRODYNAMICS OF A FRACTURE-FACIAL DOMAIN

We consider three components that make up total water content. The matrix, or M component, comprises the internal matrix pores. Microcavities on internal fracture faces make up a second component, labeled C. This could include the possibility of dead-end fractures within the matrix that are small enough to fill by capillarity under realistic high (but negative) matric potential, and that open to a fracture face. Free-surface films on internal fracture faces make up the third component, labeled F. The C and F regimes comprise the fracture-facial domain. Figure 12.1 illustrates the spatial relationships of these domains and their dynamics during and after an incidence of preferential flow from a source higher up in the profile.

In the matrix domain, capillary relations govern the moisture state as in traditional unsaturated flow theory, with matric potential as the controlling influence. The M-domain water content may be considered as the diffuse-domain water content θ_D of the source-responsive flux model [*Nimmo*, 2010]. Similarly, the F-domain water content may be considered the source-responsive preferential flow domain of this model. The C domain resembles the M domain in being sensitive to capillarity but differs in the directness of its connection to the F domain.

12.2.1. The C Domain: Roughness Storage in Microcavities

The C domain is a regime of adsorptive and surface-tension influences that resembles traditional diffuse formulations of unsaturated flow. It is typically active on a seasonal timescale. Its wetness is based on water retention in the total volume of microcavities, i.e., crevices, indentations, and other roughness features in faces of fractures, macropores, and other large void spaces of a porous medium. Such features have been hypothesized by many [e.g. *Buckingham*, 1907; *Dillard et al.*, 2001] to retain a particular amount of water at given energy state. For a particular regular geometry of angular pores, *Tuller et al.* [1999, Appendix B] developed an exact model based on capillarity.

Various terms, such as "irregularities" [*Price et al.*, 2000], have been used for these individual water-containing elements. *Or and Tuller* [2000] discussed "partially filled corner flow," and also used the terms "surface roughness element" and "pit." Here we use the term *microcavities* to emphasize that it is the concave portions of roughness irregularities in which the water is held by capillary force. The concept of unsaturated roughness storage is the collective effect of all such microcavities in an unsaturated medium. *Kibbey* [2013] computed capacity of such a domain as related to surface roughness, for particular grain-surface topographies observed in electron stereomicrographs.

Sensitivity to capillary control causes the function and behavior of the C domain to resemble those of the M domain. The degree of fullness is determined by capillary relations and the matric potential at the fracture face. For several reasons, it can be useful to regard the C domain as distinct from M. One is the possibility of disequilibrium between the fracture face and internal matrix. Another is to accommodate substantial differences in the timescale of interactions with the F domain, which may be very slow for M and essentially instantaneous for C. In mathematical formulation of the C domain, areal concepts are useful in addition to volumetric concepts, whereas the M domain has a more strictly volumetric character.

Retention properties, such as the water content vs. matric pressure relation, of the collective microcavities of a natural surface in general must be determined empirically because the microcavities, like pores in a soil, have individually irregular geometries. Each microcavity has its own such relation, and for macroscopic purposes they have to be effectively averaged within a representative elementary volume.

12.2.2. The F Domain: Flow in Free-Surface Films

The F domain is a free-surface film-flow regime on fracture faces, typically active on an individual-storm timescale. Effective flow channels may sometimes occur in the form of sheets, ribbons, rivulets, etc. The F domain can be quantified using the source-responsive model of preferential flow [*Nimmo*, 2007; *Nimmo*, 2010], extended and supplemented as appropriate.

The physical description of this domain uses free-surface film concepts and quantifications of *Dragila* [1999] and *Dragila and Wheatcraft* [2001]. The mathematical formulation is based on laminar flow of water driven by gravity. Here we take it as vertical; it could be extended to other dimensions. In this chapter we are not explicitly including the possibility of waves, instabilities, or turbulence, though these can have major importance and could be incorporated in further development.

The film may also be considered equivalent to a thick film in the sense used by *Tokunaga and Wan* [2001]. Phenomenologically, the film is thick enough that the net effect of interaction between the solid surface and molecules of the liquid is negligible relative to the net effect of interaction between the liquid molecules themselves. This distinguishes it from adsorbed thin films, dominated by adhesive force between solid and liquid. Other investigators, for example *Tuller and Or* [2001], have made a similar distinction between thin and thick films.

Quantitatively, the upper limit of film thickness is estimated to be 10 to 70 microns [*Tokunaga and Wan*, 1997; *Tokunaga et al.*, 2000]. The thickness is not determined by static relationships but by the dynamic interaction of flow rate, driving force, flow geometry (e.g. slope angle), surface roughness, and properties of the liquid. For steady-state conditions with a given medium and liquid, thickness of these films depends solely on the flux of water flowing in them [*Dragila and Wheatcraft*, 2001], the same principle by which a river's volumetric flow rate determines its depth. This dependence on the inflow of water identifies the flow in such films as a source-responsive concept [*Nimmo*, 2010]. Flux/thickness compensating mechanisms as discussed by *Nimmo* [2007] may keep the thickness within a narrow range. *Su et al.* [2003] provide a well-documented example with measured flow characteristics.

The porosity of the F-domain, ϕ_F, would equal a maximum possible effective film thickness multiplied by the fracture facial area density. This density, symbolized M, is the total area of activatable fracture internal surface area per bulk volume of rock. This porosity would typically be a small fraction of the total fracture porosity since the fracture internal space occupied by air is not part of the F-domain. The water content θ_F would essentially equal ϕ_F multiplied by the fracture active area fraction, f. *Nimmo* [2010] defined f as a number between 0 and 1 that represents the fraction of area potentially available for film flow that is actually occupied by flowing films at the time of observation.

Based on laminar flow theory the thickness of the flowing films can be calculated from

$$L = \sqrt{\frac{3\nu < v_z >}{g \cos \beta}} \qquad (12.1)$$

where $<v_z>$ is the average flow rate of water in the film (dimensions LT^{-1}), β is the inclination angle of the fractures from vertical, υ is the kinematic viscosity of the flowing fluid, and g is the acceleration of earth gravity

[*Bird et al.*, 2002, p. 46]. In a porous medium, $<v_z>$ is not normally a quantity that is known or predicted. A formula in terms of q_F, the F-domain flux density at a given depth (i.e., preferential flow) would be more useful. Considering the fracture geometry implied by the macropore facial area density M, this flux density relates to film velocity as

$$q_F = ML_F < v_z > \tag{12.2}$$

so the film thickness can be expressed as

$$L_F = \left[\frac{3\nu q_F}{Mg\cos\beta} \right]^{1/3} \tag{12.3}$$

For vertical flow of water at the surface of the earth we can use

$$L_F = B\left[\frac{q_F}{M} \right]^{1/3} \tag{12.4}$$

where B (dimensions $L^{1/3}T^{1/3}$) combines the known constants into one and has a value, in SI units, equal to 6.74×10^{-3} $m^{1/3}s^{1/3}$.

12.2.3. Fracture-Face Model Based on Films and Microcavities

Actual matric potential varies continuously through space and across domain interfaces. The C and F domains, being in direct fluid contact, can be considered to have equal matric potential. The same value would also correspond to the matric potential of the edge of the matrix or fracture face, a boundary condition for the matrix. In various applications, matric potential, like other state variables, for simplicity is often taken to be uniform within matrix material. For example, it is laterally uniform for one-dimensional downward flow. In this case it would be assumed to have a single value, ψ_M. After cessation of input from above causes water to disappear from the F domain, ψ_C would approach equilibrium with the local value of ψ_M at a rate determined by properties and conditions within the bulk matrix and at the fracture face.

Key properties of this domain include the surface roughness and the fracture-facial area per unit volume M (dimensions L^{-1}) [*Nimmo*, 2010]. As mentioned above, storage and flow characteristics notably do not depend on the aperture of fractures.

Total bulk volumetric water content θ, as measurable by a volume-averaging device such as a neutron moisture probe, in principle would be

$$\theta = \theta_M + \theta_C + \theta_F. \tag{12.5}$$

This total water content would fluctuate as the input flux and the matric potential vary. Presently-available volume-average methods for measuring water content in the field are not sufficiently accurate to distinguish differences much less than 1%, so for some purposes the θ_C and θ_F contributions may be locally negligible [*Nimmo and Mitchell*, 2013]. At large scales, however, the total volume of water indicated by small θ_C and θ_F can be significant, which is central to some applications discussed below.

A useful artificial concept is the volume of water per unit facial area of fractures, L_C (dimension L). It can be interpreted as the effective average thickness of equivalent uniform film storage. Because C-domain water has a microscopically irregular distribution on a rough surface, L_C does not represent a film thickness in the way that its counterpart L_F does.

12.3. APPLICATION AND RESULTS

12.3.1. Unsaturated Zone Hydrology of the English Chalk

The materials and setting of the English Chalk formation permit simplifications that clarify the roles played by the M, C, and F domains. In the southeast of England, the Chalk is a fine-grained (generally less than 10 μm), pure (more than 98% CaCO3), soft, white fractured limestone with some marls and flints. The unsaturated zone thickness can be 100 m or more. The region has a humid temperate climate with precipitation throughout the year. With high evapotranspiration in summer, recharging fluxes are greater in winter.

The matrix material typically has porosity of 25% to 40% [*Lewis et al.*, 1993]. Its saturated hydraulic conductivity is typically 2 to 6 mm/d [*Price et al.*, 1976; *Lee et al.*, 2006]. Pore throats of chalk matrix are small, typically less than 1 μm, giving it an extreme air-entry value, about –250 kPa or less [*Price et al.*, 2000]. This air-entry value, in combination with the wet climate and the effect of interspersed impeding layers, allows the matrix water content to be effectively saturated in many circumstances. This high saturation of the fine-pored matrix facilitates studies of fracture flow by minimizing the influence of matrix pore-water dynamics.

The fracture porosity is typically about 1% to 2% [*Lewis et al.*, 1993]. *Price et al.* [2000] present evidence from techniques of resin impregnation coupled with electron microscopy, and acoustic measurements under varying levels of stress applied to samples, that the fracture apertures are in general greater than 30 μm. This criterion chiefly applies to fractures that actively participate in preferential flow; there are known to be smaller fracturelike openings that are dead-ended or otherwise too poorly connected for significant flow.

12.3.2. Recharge During Unsaturated Conditions

There is considerable evidence that recharge by preferential flow mechanisms can occur through unsaturated chalk, observed for example from water table fluctuations. This includes the results of *Lee et al.* [2006], which *Malek-Mohammadi and Nimmo* [in review] treated with a source-responsive flux model. During a five-week interval during the winter of 2006–2007 at East Ilsley, *Gallagher et al.* [2012, their Figure 9] observed a marked increase in water table rise while matric potentials remained negative in the unsaturated zone. *Lewis et al.* [1993], in Chalk catchment water balance studies, combined and compared streamflow, recharge, water-table fluctuation, and unsaturated-zone flow dynamics on a seasonal basis. They found streamflow to be greater, by as much as a factor of 10, than could be accounted for by the recession of the water table. The discrepancy could not be explained by the drainage from the matrix, which stays effectively saturated. They estimated that drainage during one dry season, additional water equivalent to around 0.25% to 0.30% of the volume of rock in the unsaturated zone, would be sufficient to compensate for the unexpectedly small apparent contribution from the aquifer.

Price et al. [2000] showed that irregularities on fracture surfaces provide a storage capacity in the chalk unsaturated zone sufficient to account for volumes of water of the order of those required to explain the findings of *Lewis et al.* [1993]. Their laboratory experiments included water retention measurements, discussed below, that *Low et al.* [1997] presented in detail. Results showed no matrix pores that drain and fill under natural conditions. They also found that large pores (up to about 100 μm diameter, mostly in the form of foram tests) do commonly exist, but their interconnections are very small and so do not allow drainage from the matrix. On fracture faces, however, these large pores constitute microcavities of the C domain.

12.3.3. Conceptual Model

12.3.3.1. Damping depth and continuous flux

When water moves downward by diffusive unsaturated-flow processes combined with gravity, temporal fluctuations of infiltration at the land surface can be damped to the extent that the downward flux, and hence the unsaturated hydraulic conductivity and water content, are constant [*Gardner*, 1964; *Nimmo et al.*, 1994]. In the English Chalk, multiseason tensiometer measurements show the matric potential becoming constant at depths of 2 to 7 m [*Wellings and Bell*, 1980; *Wellings*, 1984]. Given water table depths typically of tens of meters, this allows for a substantial thickness of unsaturated zone to be immune from variation of diffuse fluxes in the matrix. The extreme air-entry value of the Chalk matrix means that the matrix water content would not only be constant but would be effectively saturated, which would likely further enhance its temporal stability. The low matrix hydraulic conductivity of chalk also promotes stability and shallowness of damping depth. This picture implies that preferential flow occurs within fractures and interacts minimally with matrix material, so the English Chalk affords opportunity for investigation of unsaturated preferential flow in isolation from other flow modes.

The distribution of matric potential is likely to follow patterns as observed by *Rutter et al.* [2012]. In winter when the recharging flux is large, matric potential commonly is near zero, especially in the zones just above impeding layers. In particular, matric potential becomes high above marls and may have lower values (but still within AEV) above that region up to the next marl. In drier seasons, it is likely to go to tens of kPa negative. Thus, the matric potential typically undulates with depth, but the gradient on average, from the damping depth to the water table, is essentially zero. Therefore, gravity-driven flow through the effectively saturated matrix creates an ongoing steady component of recharging flux, whose value numerically equals the saturated hydraulic conductivity of the matrix material, typically a few millimeters per year.

12.3.3.2. Flow dynamics on storm and seasonal timescales

During periods when infiltration substantially exceeds ET, downward flux at the damping depth may exceed the steady component of recharge flux through the matrix. This establishes the necessary condition to drive preferential flow by source-responsive processes through the unsaturated zone below this level. This flux in excess of the matrix flux then constitutes the flow rate that determines the thickness L_F of free-surface films in the F domain (Equations 12.1 and 12.2). Evidence from borehole video shows clear evidence of substantial film flow on borehole walls [*Gallagher et al.*, 2012]. Assuming natural fracture faces behave like the observed walls, it is likely that similar films occur in fractures. Tensiometers in boreholes for continuous monitoring have shown the matric potential increases above -5 kPa during the winter wet season, with the matrix, which is saturated at these potentials, unable to absorb water that flows down the fractures to the water table.

12.3.4. Seasonal Storage in Microcavities

Water retention properties of the C domain can be estimated using water retention data of *Low et al.* [1997]. They used a pressure-plate apparatus to measure the water content of chalk samples at a series of matric potentials. The samples came from two different quarries and varied in size and surface roughness. Some samples had naturally rough faces, being either natural fracture faces or exposed by fracturing. Others had surfaces cut smooth in sample preparation. The interior of the block is the matrix material, while the block's total outer surface area effectively acts as fracture facial area. At the start, the samples were totally saturated with water, and remaining F-domain water was allowed to drain away under gravity. The pressure-plate measurements involved static equilibrium without film flow, so water retained at the block surfaces would be in the C but not the F domain. Over the range of pressures applied, down to -150 kPa or further, the matrix remained above the air-entry value and stayed saturated, so that changes result from the dynamics of the C domain. The measured changes in sample weight during the decreasing sequence of matric potentials then indicate changes in C-domain water content.

Both *Low et al.* [1997] and *Price et al.* [2000] presented results in terms of degree of saturation of the sample volume. We similarly computed θ_C for each sample at each ψ in the measured range, with results shown in Figure 12.2 (top). Equivalent to the results published by *Low et al.* [1997] and *Price et al.* [2000], these are plotted on a relative scale that indicates the change in C-domain water from its amount at −160 kPa.

It is instructive to relate this water content change to what it implies concerning the total water storage in the unsaturated-zone volume of the catchment, as done by *Price et al.* [2000]. In doing so it must be kept in mind that additional factors may become significant when moving from the small and perhaps idealized lab samples to the entire catchment. The relevant calculation is of the amount of water released from a large volume of fractured chalk during a seasonal decline of matric potential. Considering seasonal variations of matric potential in the Chalk between −1 kPa during winter to −50 kPa or less during summer, the average effective storage capacity of the C domain is about 0.4%. This value is consistent with estimates of 0.25% to 0.35% that *Lewis et al.* [1993] had calculated would be needed to permit enough seasonal storage in the deep unsaturated zone to explain the observation of high dry-season streamflow with minimal water table recession.

With additional assumptions we can calculate the water retention on an areal basis, i.e., the volume of water per unit area of sample face, equal to L_C, as a function of matric potential. Like the original investigators, we assume no major internal fractures, though there may be dead-end microfractures that contribute to storage but not rapid flow. We estimate the outer surface area of samples from the reported sample volumes. Geometrically, for a given shape, regardless of size, the ratio of the square root of the area to the cube root of the volume is the same. Thus, the outer area of a block is

$$A = GV^{2/3} \tag{12.6}$$

where V is the bulk volume of the block and G is a geometric factor, the surface area to volume ratio, that has a characteristic constant value for each type of shape. For spheres and cubes, which have known surface area and volume formulas, it is easy to determine that G equals 4.84 and 6, respectively. Its value is greater for more elongated or more irregular shapes. For the somewhat elongated, somewhat irregular shapes of the samples of *Low et al.* [1997], we assume G equals 8. This gives the values in Table 12.1. The facial area per unit volume M is the ratio of the estimated area from Equation 12.6 to the bulk volume in this table. Using the computed M values from Table 12.1 and

$$\theta_C(\psi) = ML_C(\psi) \tag{12.7}$$

we also computed effective L_C for each sample at each ψ in the range (Figure 12.2, bottom). Again considering the change in retained water over a −1 kPa to −50 kPa range, the change in L_C would be about 40 μm for sample SH5/5 and about 20 μ for others. These numbers are approximate, in particular because of uncertainty of L_C at the wet end of the range.

It is interesting to compare L_C with results of *Weisbrod et al.* [2000], who measured root-mean-square roughness about 100 to 200 μm for uncoated chalk surfaces, and *Price et al.* [2000], whose photomicrographs suggest that foram tests cause a similar or somewhat lesser degree of roughness. Note that these values, representing indentations from the fracture face, can be larger than the fracture's aperture. Our L_C estimates of 20–40 μm are consistent with such roughness, given that L_C represents an average equivalent film thickness, as if water from microcavities were evenly spread over the entire surface.

Interpretation of the retention data on the areal basis here differs from some of the volume-based interpretations of *Price et al.* [2000], though it also supports the hypothesis of significant roughness storage. The L_C interpretation allows comparison of D domain water per unit area of fracture face, thus characterizing the material of the different samples. Three samples show very similar C-domain characteristics and the fourth indicates significantly greater retention over the range. Systematic differences on the basis of natural vs. smooth-cut surfaces and small vs. large samples are not apparent. Instead there is a distinction between the three samples from one quarry (PH), and the single one, with greater retention, from the other (SH). Though four samples cannot establish much confidence, this suggests a possible innate material difference in samples from the different chalk formations.

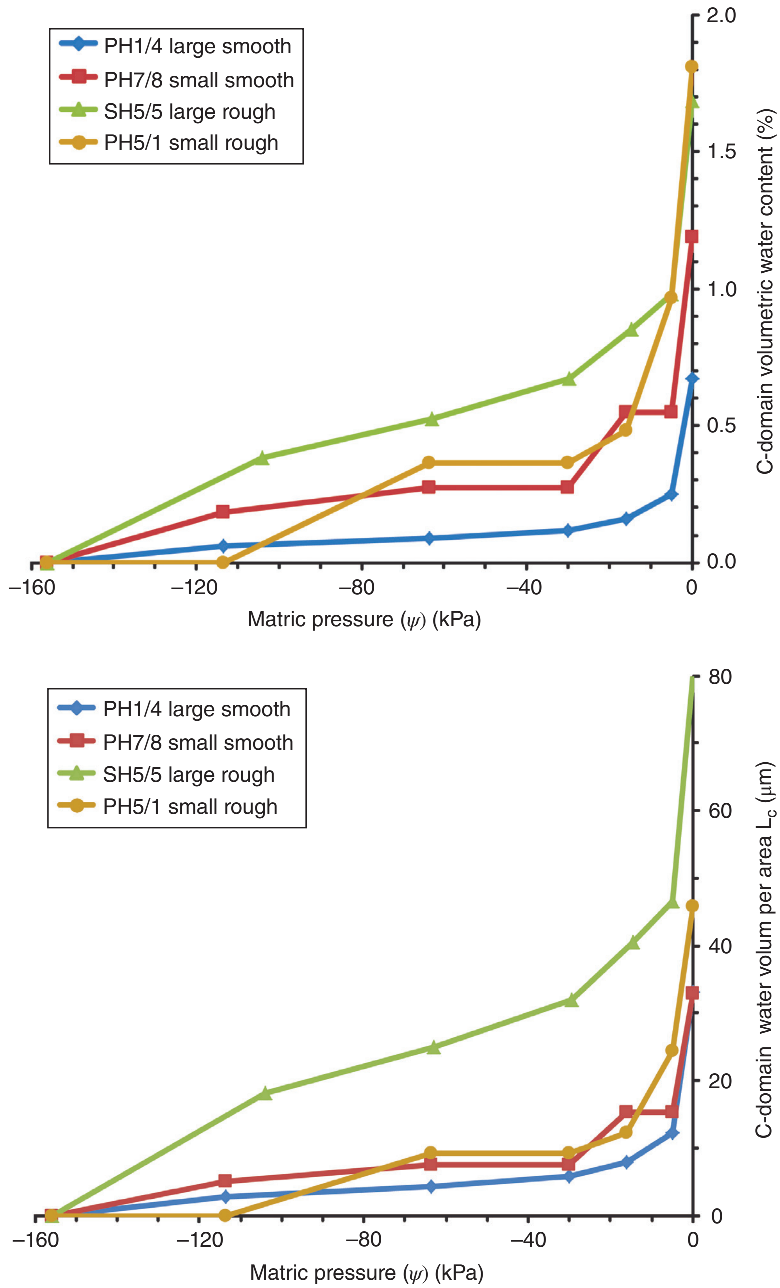

Figure 12.2 Microcavity (C-domain) water retention for four samples measured by *Low et al.* [1997]. Top: Volumetric basis, indicating the volume of C water per bulk volume of material. Bottom: Areal basis, indicating the volume of C water per unit facial area of fracture faces.

Table 12.1 Volumes and areas of four samples used for water retention measurements by *Low et al.* [1997]. The designations "PH1/4" etc. are the published sample labels. The samples are from two different quarries, PH and SH.

Sample	Bulk Volume (cm^3)	Estimated Area (cm^2)	M (m^{-1})
PH1/4 large smooth	68.65	139	203
PH7/8 small smooth	10.93	39	360
SH5/5 large rough	55.18	116	210
PH5/1 small rough	8.29	33	395

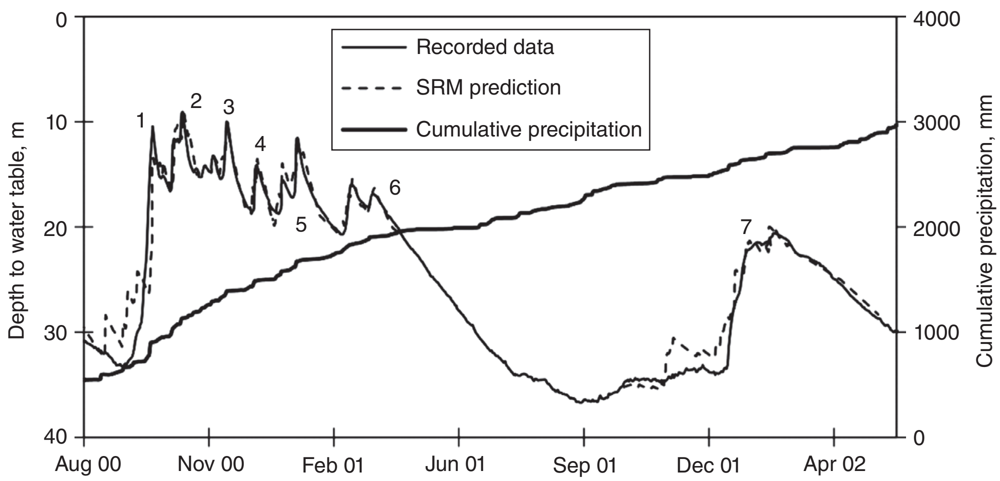

Figure 12.3 Measured and predicted water table and precipitation over a 22-month period at the Houndean site [*Lee et al.,* 2006]. Predictions were made by *Malek-Mohammadi and Nimmo* [in review] using the source-responsive flux model.

12.3.5. Film Flow

Malek-Mohammadi and Nimmo [in review] successfully applied the source-responsive flux model [*Nimmo*, 2010] to predict the fast water-table response at two sites located in the Upper and Middle Chalk, Broadhalfpenny, and Houndean. The simulated water level is compared with the field-recorded data provided by Lee et al. [2006] as shown in Figure 12.3. In most rapid-rise cases, the model predicts the final peak and timing with good accuracy. The model provides a practical tool for estimating a physically reasonable upper bound on possible recharge for the Upper and Middle Chalk. The simulation results also demonstrate that this model can be employed in a continuous mode to quantify the dominant recharge process over annual timescales. Optimized M values from the model calibration were about 300 m^{-1}, in good general agreement with our estimates of M (Table 12.1) from the data of *Low et al.* [1997].

12.4. DISCUSSION

12.4.1. Hydrologic Role of Roughness Storage and Film Flow

The three-domain matrix-microcavity-film model presented here usefully organizes the properties and relationships of the components of an unsaturated fractured-rock system. The collective results of physical property and flux evaluations in the English Chalk unsaturated zone support the model and its applicability.

These results suggest some new directions for thinking about unsaturated flow in fractured rocks. The model conceptually distinguishes (1) a mostly static, capillarity-governed facial storage domain, whose key variable is the matric potential at the fracture face, and (2) a flow domain with water content governed by free-surface film-flow relations, whose key variable is the flux supplied to the domain. Both of these facial domains are distinct from the matrix domain, from which they differ in degree of mobility and timescale of interaction. The model identifies hydraulic properties and relationships for these unsaturated fracture-facial domains and underlines their hydrologic significance.

The domain of microcavities accommodates significant water storage within the unsaturated zone on an intermediate timescale. Water seasonally stored in the unsaturated zone in this way does not fall under the definition of recharge because it is not yet in the aquifer. As hypothesized by *Price et al.* [2000], It may contribute to streamflow in the same manner as aquifer water, though given the possibility of rapid lateral transport, it may have too short a residence time in the saturated zone to register as a measurable rise of water table. This can be responsible for the minimal seasonal decline of streamflow despite the drastically different behavior of water table recession curves during wet and dry seasons as in Figure 12.3.

12.4.2. Reinitiation of Preferential Flow

This model also suggests possible mechanisms for reinitiation of preferential flow after temporary cessation, which would help to explain observations of long-range preferential flow through deep unsaturated zones [*Pruess*, 1999]. It is paradoxical how preferential flow can persist for years, taking tracers to depths of hundreds of meters while the rock remains unsaturated. The source-responsive travel-time model [*Nimmo*, 2007] hypothesizes pulsed preferential flow when the water source is intermittent, and requires there be a mechanism to reactivate preferential flow. The behavior of marls noted by *Rutter et al.* [2012], in acting to generate seepage and free-surface film flow [*Su et al.*, 2003], suggests analogous processes may occur where there are layers of contrasting impedance. Reactivation after a period of zero flux in the F domain could also be triggered by a pressure pulse that propagates downward with the initial pulse of a new infiltration episode. Such a mechanism could explain how a source-responsive model would apply to deep unsaturated zones as by *Ebel and Nimmo* [2013] and *Mirus and Nimmo* [2013].

12.4.3. Further Possible Extensions

Dynamics of the M, C, and F domains could also enhance understanding of solute transport. C-domain water, which may include contaminants from the land surface brought to depth by flow in the F domain, may remain in the unsaturated zone long enough for diffusion to carry solutes into the matrix. This process might considerably enhance contaminant transport into the matrix at depth compared to what is transported by slow matrix flow or by the fast and temporary F-domain water. Such a mechanism may be responsible for some bypass of matrix material observed by *Smith et al.* [1970], who found 15% of bomb tritium in the matrix pore water to reside at depths lower than was possible by matrix transport alone. The conclusion drawn from this was that while flow in the Chalk is dominated by diffusive flow, 15% of it is transported through fractures. *Foster and Smith-Carington* [1980] suggested that high tritium concentration recorded in pores might occur as a result of diffusion from fractures to matrix domain. The three-domain model presented here can clarify and help resolve such issues.

It is possible to develop models analogous to the capillary-bundle models commonly used for flow describable by Darcy's law or Richards' equation. Similar to the model of *Or and Tuller* [2000], one could postulate a regularized geometry, for example, conical pits varying in diameter or angle, in the way that capillaries are used for soil pores, and from the measured retention curve, calculate a corresponding distribution of diameters or angles that would give that curve.

12.5. CONCLUSIONS

A fracture-facial region of the pore space, with a combination of a flowing phase whose fullness is determined by the availability and flux of preferentially flowing water, and a slower-changing portion whose fullness is determined by the local matric potential, can have explanatory value for the hydrodynamics of a hydrologic system that includes unsaturated fractured rock. Rough fracture surfaces can provide storage that operates on a seasonal timescale, even while its replenishing fluxes operate on an individual-storm timescale. Microcavities on fracture faces and their capability to store the percolating water creates conditions suitable for the water and contaminants to be exchanged between the two domains by diffusion.

While the long-term water table response in the Chalk is controlled by the matrix flow (M domain), source-responsive models can represent the characteristic behavior of rapid water table response during unsaturated conditions (F domain) [*Malek-Mohammadi and Nimmo*, in review]. The model also highlights the importance of C-domain water, stored during winter (near-zero matric potential), which gradually drains to the aquifer during summer (lower matric potentials), reducing the apparent water table recession.

This model should be applicable to other sites and media. These often would have a less uniform or coarser-pored matrix, making it more difficult to identify the specific features involved. However, the same principles can be applied, and the mathematical formulation may be valuable even if the processes are not so easily distinguishable.

Estimated properties and parameter values for the three-domain matrix-microcavity-film model are consistent with quantitative information from diverse sources. The model provides a way to link together in a consistent picture such quantities as recharge estimates, streamflow, water table fluctuation, analysis of surface roughness, imaging by electron microscopy, and surface roughness. The self-consistency of this model, and its consistency with a body of diverse data in the English Chalk, supports the hypothesized active mechanisms of the three domains and establishes the usefulness of this framework.

REFERENCES

Bird, R. B., W. E. Stewart, and E. N. Lightfoot (2002), *Transport Phenomena*, Wiley, New York.

Buckingham, E. (1907), Studies on the movement of soil moisture, *USDA Bureau of Soils Bulletin*, *38*.

Celia, M. A., P. C. Reeves, and L. A. Ferrand (1995), Recent advances in pore scale models for multiphase flow in porous media, *Reviews of Geophysics*, *33*(S2), 1049–1057.

Dillard, L. A., H. I. Essaid, and M. J. Blunt (2001), A functional relation for field-scale nonaqueous phase liquid dissolution developed using a pore network model, *Journal of Contaminant Hydrology*, *48*(1–2), 89–119, doi:10.1016/S0169-7722(00)00171-6.

Dragila, M. I. (1999), A new theory for transport in unsaturated fractures: Free surface film flows, University of Nevada, Reno, Ph.D. Dissertation.

Dragila, M. I., and N. Weisbrod (2003), Parameters affecting maximum fluid transport in large aperture fractures, *Advances in Water Resources*, *26*(12), 1219–1228.

Dragila, M. I., and S. W. Wheatcraft (2001), Free-surface films, in *Conceptual Models of Flow and Transport in the Fractured Vadose Zone*, pp. 217–241, National Academy Press, Washington, DC.

Ebel, B. A., and J. R. Nimmo (2013), An alternative process model of preferential contaminant travel times in the unsaturated zone: Application to Rainier Mesa and Shoshone Mountain, Nevada, *Environmental Modeling and Assessment*, *18*(3), 345–363, doi:10.1007/s10666-012-9349-8.

Foster, S., and A. Smith-Carington (1980), The interpretation of tritium in the Chalk unsaturated zone, *Journal of Hydrology*, *46*(3), 343–364.

Gallagher, A. J., H. K. Rutter, D. K. Buckley, and I. Molyneux (2012), Lithostratigraphic controls on recharge to the Chalk aquifer of Southern England, *Quarterly Journal of Engineering Geology and Hydrogeology*, *45*(2), 161–172, doi:10.1144/1470-9236/09-048.

Gardner, W. R. (1964), Water movement below the root zone, *Transactions, 8th International Congress of Soil Science*, 63–68, International Society of Soil Science, Bucharest, Romania.

Hincapié, I. A., and P. F. Germann (2009), Abstraction from infiltrating water content waves during weak viscous flows, *Vadose Zone Journal*, *8*(4), 891–901.

Kibbey, T. C. G. (2013), The configuration of water on rough natural surfaces: Implications for understanding air-water interfacial area, film thickness, and imaging resolution, *Water Resources Research*, *49*(8), 4765–4774, doi:10.1002/wrcr.20383.

Lee, L. J. E., D. S. L. Lawrence, and M. Price (2006), Analysis of water-level response to rainfall and implications for recharge pathways in the Chalk aquifer, SE England, *Journal of Hydrology*, *330*(3–4), 604–620.

Lewis, M. A., H. K. Jones, D. M. J. Macdonald, M. Price, J. A. Barker, T. R. Shearer, A. J. Wesselink, and D. J. Evans (1993), Groundwater storage in British aquifers—Chalk, *National Rivers Authority R&D Note*, *169*, Bristol, UK.

Low, R. G., C. McCann, and M. Price (1997), Mechanisms of water storage in the unsaturated zone of the Chalk aquifer, *Environment Agency R&D Technical Report*, *W50*, Bristol, UK.

Malek-Mohammadi, S., and J. R. Nimmo (in review), Preferential flow and water storage dynamics in unsaturated fissures: Case study in the English Chalk, *Hydrological Processes*.

Mirus, B. B., and J. R. Nimmo (2013), Balancing practicality and hydrologic realism: A parsimonious approach for simulating rapid groundwater recharge via unsaturated-zone preferential flow, *Water Resources Research*, *49*(3), 1458–1465, 2012WR012130, doi:10.1002/wrcr.20141.

Nimmo, J. R. (2007), Simple Predictions of maximum transport rate in unsaturated soil and rock, *Water Resources Research*, *43*(5), W05426, doi:10.1029/2006wr005372.

Nimmo, J. R. (2010), Theory for source-responsive and free-surface film modeling of unsaturated flow, *Vadose Zone Journal*, *9*(2), 295–306.

Nimmo, J. R. (2012), Preferential flow occurs in unsaturated conditions, *Hydrological Processes*, *26*(5), 786–789.

Nimmo, J. R., and L. Mitchell (2013), Predicting vertically nonsequential wetting patterns with a source-responsive model, *Vadose Zone Journal*, *12*(4), doi:10.2136/vzj2013.03.0054.

Nimmo, J. R., D. A. Stonestrom, and K. C. Akstin (1994), The feasibility of recharge rate determinations using the steady-state centrifuge method, *Soil Science Society of America Journal*, *58*(1), 49–56.

Or, D., and M. Tuller (1999), Liquid retention and interfacial area in variably saturated porous media: Upscaling from single-pore to sample-scale model, *Water Resources Research*, *35*(12), 3591–3605, doi:10.1029/1999wr900262.

Or, D., and M. Tuller (2000), Flow in unsaturated fractured porous media: Hydraulic conductivity of rough surfaces, *Water Resources Research*, *36*, 1165–1177.

Price, M., M. J. Bird, and S. S. D. Foster (1976), Chalk pore-size measurements and their significance, *Water Services*, *80*(968), 596–600.

Price, M., R. G. Low, and C. McCann (2000), Mechanisms of water storage and flow in the unsaturated zone of the Chalk aquifer, *Journal of Hydrology*, *233*(1–4), 54–71.

Pruess, K. (1999), A mechanistic model for water seepage through thick unsaturated zones in fractured rocks of low matrix permeability, *Water Resources Research*, *35*(4), 1039–1051.

Rutter, H. K., J. D. Cooper, D. Pope, and M. Smith (2012), New understanding of deep unsaturated zone controls on recharge in the Chalk: A case study near Patcham, SE England, *Quarterly Journal of Engineering Geology and Hydrogeology*, *45*(4), 487–495, doi:10.1144/qjegh2011-010.

Smith, D. B., P. L. Wearn, H. J. Richards, and P. C. Rowe (1970), Water movement in the unsaturated zone of high and low permeability strata by measuring natural tritium, *Isotope Hydrology*, *IAEA-SM-129*(6), 73–87.

Su, G. W., J. T. Geller, K. Pruess, and F. Wen (1999), Experimental studies of water seepage and intermittent flow in unsaturated, rough-walled fractures, *Water Resources Research*, *35*(4), 1019–1037.

Su, G. W., J. R. Nimmo, and M. I. Dragila (2003), Effect of isolated fractures on accelerated flow in unsaturated porous rock, *Water Resources Research*, *39*(12), 1326, doi:10.1029/2002wr001691.

Tokunaga, T., and J. Wan (1997), Water film flow along fracture surfaces of porous rock, *Water Resources Research*, *33*(6), 1287–1295.

Tokunaga, T. K., and J. Wan (2001), Approximate boundaries between different flow regimes in fractured rocks, *Water Resources Research*, *37*(8), 2103–2111.

Tokunaga, T. K., J. Wan, and S. R. Sutton (2000), Transient film flow on rough fracture surfaces, *Water Resources Research*, *36*(7), 1737–1746.

Tuller, M., and D. Or (2001), Hydraulic conductivity of variably saturated porous media: Film and corner flow in angular pore space, *Water Resources Research*, *37*(5), 1257–1276.

Tuller, M., D. Or, and L. M. Dudley (1999), Adsorption and capillary condensation in porous media: Liquid retention and interfacial configurations in angular pores, *Water Resources Research*, *35*(7), 1949–1964.

Weisbrod, N., R. Nativ, E. M. Adar, D. Ronen, and A. Ben-Nun (2000), Impact of coating and weathering on the properties of chalk fracture surfaces, *Journal of Geophysical Research: Solid Earth*, *105*(B12), 27853–27864, doi:10.1029/2000jb900295.

Wellings, S. R. (1984), Recharge of the upper chalk aquifer at a site in Hampshire, *England, Journal of Hydrology*, *69*, 259–273.

Wellings, S. R., and J. P. Bell (1980), Movement of water and nitrate in the unsaturated zone of upper chalk near Winchester, Hants., *England, Journal of Hydrology*, *48*, 119–136.